

RECEIVED BY OSTI

JAN 07 1986

CONF-860135-1

UCRL-93778  
PREPRINT

**AIR QUALITY MODELING FOR  
EMERGENCY RESPONSE APPLICATIONS**

**P. H. Gudiksen  
S. T. Chan  
J. B. Knox  
M. H. Dickerson  
R. Lange**

To be presented to the Indian Science Congress  
Annual Session: Symposium on "Recent Advances  
in the Development of Numerical Models for the  
Dispersion of Atmospheric Pollutants"

January 4-5, 1986.

December, 1985

Lawrence  
Livermore  
National  
Laboratory

This is a preprint of a paper intended for publication in a journal or proceedings. Since changes may be made before publication, this preprint is made available with the understanding that it will not be cited or reproduced without the permission of the author.

MASTER

## DISCLAIMER

This report was prepared as an account of work sponsored by an agency of the United States Government. Neither the United States Government nor any agency thereof, nor any of their employees, makes any warranty, express or implied, or assumes any legal liability or responsibility for the accuracy, completeness, or usefulness of any information, apparatus, product, or process disclosed, or represents that its use would not infringe privately owned rights. Reference herein to any specific commercial product, process, or service by trade name, trademark, manufacturer, or otherwise does not necessarily constitute or imply its endorsement, recommendation, or favoring by the United States Government or any agency thereof. The views and opinions of authors expressed herein do not necessarily state or reflect those of the United States Government or any agency thereof.

UCRL--93778

DE86 004629

## AIR QUALITY MODELING FOR EMERGENCY RESPONSE APPLICATIONS

P. H. Gudiksen, S. T. Chan, J. B. Knox

M. H. Dickerson and R. Lange

Lawrence Livermore National Laboratory

University of California

Livermore, California

## ABSTRACT

The three-dimensional diagnostic wind field model (MATHEW) and the particle-in-cell transport and diffusion model (ADPIC) are used by the Atmospheric Release Advisory Capability (ARAC) for real-time assessments of the consequences from accidental releases of



radioactivity into the atmosphere. For the dispersion of hazardous heavier-than-air gases, a time- dependent three-dimensional finite element model (FEM3) is used. These models have been evaluated extensively against a wide spectrum of field experiments involving the release of chemically inert tracers or heavier- than-air gases. The results reveal that the MATHEW/ADPIC models are capable of simulating the spatial and temporal distributions of tracer concentration to within a factor of 2 for 50% of the measured tracer concentrations for near surface releases in relatively flat terrain and within a factor of 2 for 20% of the comparisons for elevated releases in complex terrain. The FEM3 model produces quite satisfactory simulations of the spatial and temporal distributions of heavier-than-air gases, typically within a kilometer of the release point.

The ARAC consists of a centralized computerized emergency response system that is capable of supporting up to 100 sites and providing real-time predictions of the consequence of transportation accidents that may occur anywhere. It utilizes pertinent accident information, local and regional meteorology, and terrain as input to the MATHEW/ADPIC models for the consequence analysis. It has responded to over 150 incidents and exercises over the past decade.

## INTRODUCTION

A variety of air quality models are currently in use to address emergency response applications. In general, the models may be divided into three generic categories. These are: (1) Gaussian models, (2) sequential puff models, and (3) three-dimensional models. For a variety of simple cases, the Gaussian models can provide dose estimates out to 5-10 km from the source point based on little meteorological information, with the distance depending on the complexity of the terrain and meteorology. The sequential puff models accept meteorological data from a multitude of measurement sites to provide more realistic estimates of plume trajectory and concentration patterns for distances beyond 5-10 km. With the advent of improved computing capabilities, advanced three-dimensional models have come into more general use. These models have the capability to directly include wind

direction and speed shears in both horizontal and vertical directions and terrain effects as well as parameterizations of deposition, surface roughness, and variable atmospheric stability in the vertical direction.

The DOE sponsored atmospheric research activities at LLNL have been directed toward (1) the development of three-dimensional diagnostic models with specific application to real-time nuclear emergency response, and (2) the development of a three-dimensional time-dependent model based on the finite element methodology for simulating atmospheric transport and diffusion of heavier-than-air hazardous substances. This paper provides an overview of the three-dimensional diagnostic wind field model (MATHEW) and the particle-in-cell atmospheric transport and diffusion model (ADPIC) that are used by the Atmospheric Release Advisory Capability (ARAC) to estimate the consequences of accidental releases of radioactivity into the atmosphere,[1,2,3]. This includes a summary of their extensive evaluations against field experiments conducted in a variety of environmental settings, a description of the most recent Atmospheric Studies in Complex Terrain (ASCOT) field experiments designed to improve and evaluate the models, and an overview of the ARAC project. In addition, the paper includes a description of the three-dimensional time-dependent finite element model (FEM3) and its evaluation using data from field experiments involving heavier-than-air gas spills.[4]

#### DESCRIPTION OF MATHEW/ADPIC MODELS

The MATHEW/ADPIC models are coupled. MATHEW is a diagnostic model which interpolates surface and upper air wind observations to produce a three-dimensional gridded wind field that is made mass conservative by a variational technique based on a least squares adjustment of the winds in the presence of terrain.[1] Thus, the mass conservative wind field generated by MATHEW is based on time averaged wind observations, the complexity of the underlying terrain and the atmospheric stability. This wind field is used to drive the ADPIC model, which is a three-dimensional particle-in-cell transport and diffusion model that calculates the time-dependent dispersion of inert or radioactive pollutants

under complex conditions[2,5]. It utilizes thousands of Lagrangian "mass" particles to represent the pollutant. These are transported inside a fixed Eulerian grid. The model solves the three-dimensional advection-diffusion equation in flux conservative form,

$$\frac{\partial \chi}{\partial t} + \nabla \cdot (\chi \vec{U}_p) = 0 \quad (1)$$

where  $\chi$  is the pollutant concentration and  $\vec{U}_p$  is a velocity which is defined as the sum of the mean wind  $\vec{U}_A$  and a diffusive velocity  $\vec{U}_D$

$$\vec{U}_p = \vec{U}_A + \vec{U}_D; \vec{U}_D = -K \frac{\nabla \chi}{\chi} \quad (2)$$

and  $K$  is the diffusivity in the  $x$ ,  $y$ , and  $z$  directions.  $U_A$  is supplied by the MATHEW model. ADPIC computes a horizontal and a vertical diffusivity  $K_h$  and  $K_z$ . The  $K_h$  is based on the following relationship

$$K_h = \sigma_y \frac{d\sigma_y}{dt} \quad (3)$$

where  $\sigma_y$  is the horizontal standard deviation of the plume. For plumes,  $\sigma_y$  is based on the semi-empirical expression

$$\sigma_y = \sigma_0 U t f(t/r); \quad f(t/r) = (1 + t/r)^{-1/2} \quad (4)$$

where  $\sigma_0$  is the horizontal standard deviation of the fluctuation of the wind direction,  $U$  is the local mean wind speed,  $t$  is the time, and  $f(t/r)$  is a correlation function, similar to Draxler's, with an empirical time constant  $r$ .[6] For puffs,  $\sigma_y$  is based on Walton's scale-dependent expression.[7]

$$\sigma_y = (\sigma_0^{2/3} + 2/3 C_1 \epsilon^{1/3} t)^{3/2} \quad (5)$$

where  $\sigma_0$  is the original standard deviation of the puff distribution,  $C_1$  is a constant of the order of unity, and  $\epsilon$  is the energy dissipation rate in the atmosphere. When this relationship is substituted in the expression for the similarity theory diffusivity parameter

$$K_h = C_2 \epsilon^{1/3} (\sigma(t))^{4/3} \quad (6)$$

where  $C_2$  is an empirical constant of order unity, we obtain  $K_h$  as a function of  $\epsilon$  and time

$$K_h = C_2 \epsilon^{1/3} (\sigma_0^{2/3} + 2/3 C_1 \epsilon^{1/3} t)^2 \quad (7)$$

The value of  $\epsilon$  is acquired from the following expression provided by Priestly [8]

$$\epsilon = \frac{0.03}{z} \left( \frac{U}{5} \right)^3 \quad (8)$$

For the surface layer  $K_z$  is based on the Monin-Obukhov similarity theory.[9] In the outer atmospheric boundary layer  $K_z$  is of the form [10]

$$K_z = \frac{k U_* z}{\phi(z/L)} e^{-|V_g/U_*|z/h} \quad (9)$$

where  $k$  is the Von Karman constant,  $U_*$  is the friction velocity,  $z$  is the height,  $\phi(z/L)$  is an atmospheric stability function based on  $z$  and Monin-Obukhov scale length  $L$ ,  $V_g$  is the geostrophic wind and  $h$  is the height of the mixing layer.

#### MATHEW/ADPIC MODEL EVALUATION STUDIES

These models have undergone an extensive series of performance evaluations to ascertain their capability to simulate pollutant transport and diffusion characteristics of the atmosphere during a wide variety of meteorological and terrain situations.[11] The initial evaluations were based on meteorological and tracer data acquired by field experiments conducted in 1971 at the Idaho National Engineering Laboratory (INEL) in Idaho and at the Savannah River Plant (SRP) in South Carolina in 1974 over relatively flat terrain.[12] More recently, several additional data bases have become available. The ARAC response to the purge of Kr-85 from the TMI containment over a 12 day period in 1980 provided an opportunity to compare model predictions with field measurements in rolling terrain.[13] This was followed in 1981 by the field experiments conducted by the Electric Power Research Institute (EPRI) of the buoyant plumes generated by the Kincaid coal-fired power plant situated in flat terrain in Illinois.[14]

Our participation in the Department of Energy sponsored ASCOT program has resulted in model improvements and evaluations using data from nocturnal drainage flow

field experiments conducted in complex mountain valley settings in northern California during 1980 and 1981.[15,16] The models have also been evaluated using a series of daytime tracer experiments conducted during 1983 as part of the Mesoscale Atmospheric Transport Studies (MATS) at the SRP.[17] In addition to these studies, researchers in Italy have evaluated the models against a series of seabreeze experiments conducted at the Montalto nuclear power plant site situated about 100 km northwest of Rome, Italy[18].

These experiments utilized a multitude of tracers. These included routine emissions of Ar-41 from the SRP nuclear reactors; the controlled venting of Kr-85 from the TMI containment; I-131 releases at INEL; sulfur hexafluoride releases from the SRP, the Montalto, and Kincaid power plant sites; as well as perfluorocarbon and heavy methane releases that were part of the ASCOT experiments. The releases occurred from the 60 m stacks at the SRP and TMI, and from the 160 m stack at the Kincaid power plant. The remaining releases generally occurred near the surface except for one heavy methane tracer that was released at 60 m during the 1980 ASCOT experiments and one perfluorocarbon tracer released in a cooling tower plume during the 1981 ASCOT experiments. The duration of the releases varied from 15 min to several hours. Extensive surface sampling networks were employed in each series of experiments out to varying distances from the release point. These were typically 80 km for the 1971 SRP and 1974 INEL studies, 40 km for the EPRI and TMI studies, 30 km for the MATS experiments, 10 km for the ASCOT experiments, and approximately 6 km for the studies at Montalto, Italy. The experiments were supported by a variety of surface and upper air observations. This ranged from adequate meteorological coverage during the TMI purge of Kr-85 to a wide spectrum of measurement systems, including acoustic sounders, tethersondes, rawinsondes, optical anemometers, and towers, that were an integral part of the ASCOT experiments.

A statistical analysis of the models' performance for simulating the transport and diffusion of these tracers was acquired by deriving a factor  $R$ , which is the ratio of the calculated to measured tracer concentration at each sampler location for each experiment.

This permits one to plot the percent of the comparisons that are within any given factor  $R$  as a function of  $R$ . The results of each experiment is provided in Reference 11. The model performance associated with these experiments may be bracketed by the curves shown in Fig. 1. The best simulations of the experimental data is given by the upper curve that is associated with rolling terrain and near-surface tracer releases; while the most difficult simulations are associated with complex terrain and elevated releases. Other situations provide results that are intermediate to these curves. Hence, the best results indicate that the calculated concentrations are within a factor of 2 for 50% of the measured concentrations or within a factor of 5 for 75% of the comparisons. This degrades to 20% that are within a factor of 2 or 35% within a factor of 5 for the comparisons associated with elevated releases in complex terrain. This degradation of results in complex terrain is due to a variety of factors such as the limited representativeness of measurements in complex terrain, the limited spatial resolution afforded by the models, and the turbulence parameterizations used to derive the eddy diffusivities.

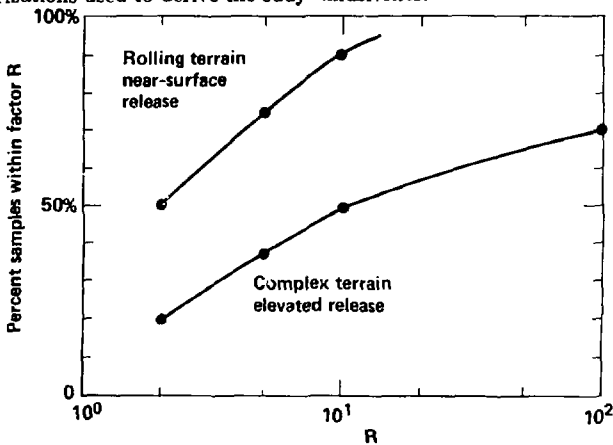


Figure 1. Percent of computed air concentrations within a factor  $R$  of measured values. The figure provides a measure of the spectrum of model evaluation results that span from near-surface tracer releases in rolling terrain to elevated releases in complex terrain.

Our current model evaluation efforts are focused on further studies on the capability of the models to simulate transport and diffusion processes associated with terrain dominated flows in complex terrain. This is presently being addressed by using the meteorological and tracer measurements acquired during the September-October 1984 ASCOT field experiments conducted in the Brush Creek valley in western Colorado.[19] This valley, situated about 55 km northeast of Grand Junction, is a narrow 25 km long valley that is oriented in a northwest-southeast direction. It is roughly 650 m deep at the south end with deep sidewall slopes of 30 - 40°. A computer generated view of this valley is shown in Fig. 2. This series included five separate experiments designed to evaluate the nocturnal valley flows as well as the flows observed during the morning transition and daytime periods. The technical objectives of these experiments were to evaluate the mass, momentum, energy, and turbulence associated with the valley and slope flows as well as to evaluate the radiative energy exchange at the surface that govern these flows. The experiments utilized a multitude of measurement systems that were fielded by over 15 different organizations. This included doppler lidar, doppler SODAR, optical anemometers, a wide variety of tower mounted meteorological instruments, and three perfluorocarbon and one oil fog tracers along with associated sampling systems.

Analysis of the data is currently underway, and a few of the main features of the valley flows have been revealed. Figure 3 shows the high spatial resolution measurements of the along valley axis flows acquired by the NOAA Wave Propagation Laboratory doppler lidar at selected times throughout the diurnal cycle. The figure depicts the velocity of the flows across a vertical plane positioned perpendicular to the valley axis. Positive and negative values indicate downvalley and upvalley flows, respectively. Note that during the nocturnal period a downvalley jet is centered over the valley as a result of the drainage down the valley slopes and from the many small tributaries. As one enters the morning transition period, the drainage jet moves toward the west sidewall because of the preferential heating of this slope during sunrise. Finally, during the daytime, one observes a general upslope

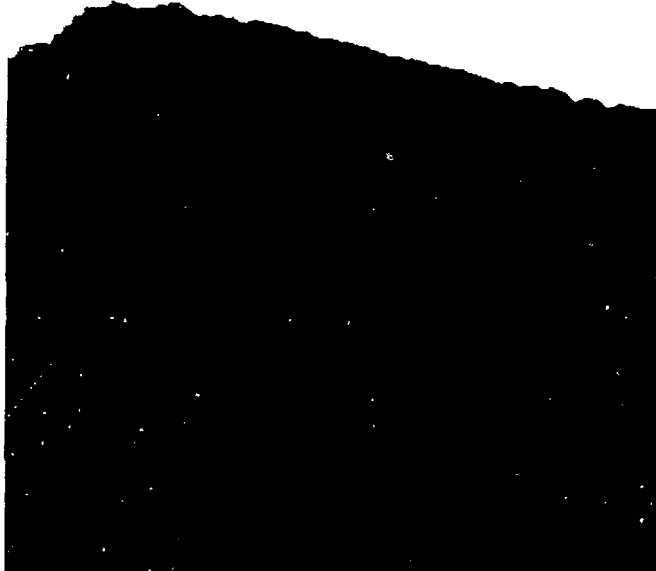


Figure 2. Computer generated depiction of the Brush Creek Valley in Western Colorado. flow regime as the valley surfaces are more uniformly heated by the sun. This general pattern is also depicted by the spatial and temporal distributions of the perfluorocarbon tracers released within the valley.

Another perfluorocarbon tracer was released on the surface of the mesa directly above a small tributary on the east side of the Brush Creek valley to evaluate the contributions of the tributary flows to the nocturnal valley flows. In order to visualize the dynamics of the flows from the mesa subsiding into the tributary and subsequently merging with the main valley flows, an oil fog tracer was released simultaneously with the perfluorocarbon tracer. The oil fog was then detected visually by time lapse photography from a vantage point. Fig. 4 shows the spatial distribution of the oil fog as it descends like a waterfall down into the tributary, disperses within the tributary and subsequently merges with the main valley flows along a streamline that rises over a hump in the terrain. Preliminary predictions by

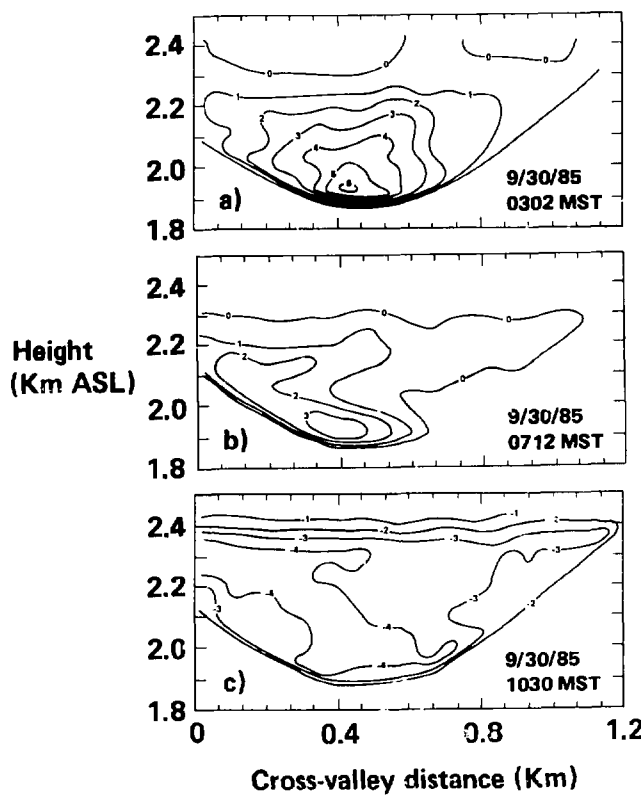


Figure 3. Vertical cross-sections of the along valley-axis flows in the Brush Creek valley during (a) the nighttime, (b) the morning transition period, and (c) the daytime. Positive values denote down-valley flows in m/s, while negative values depict up-valley flows.

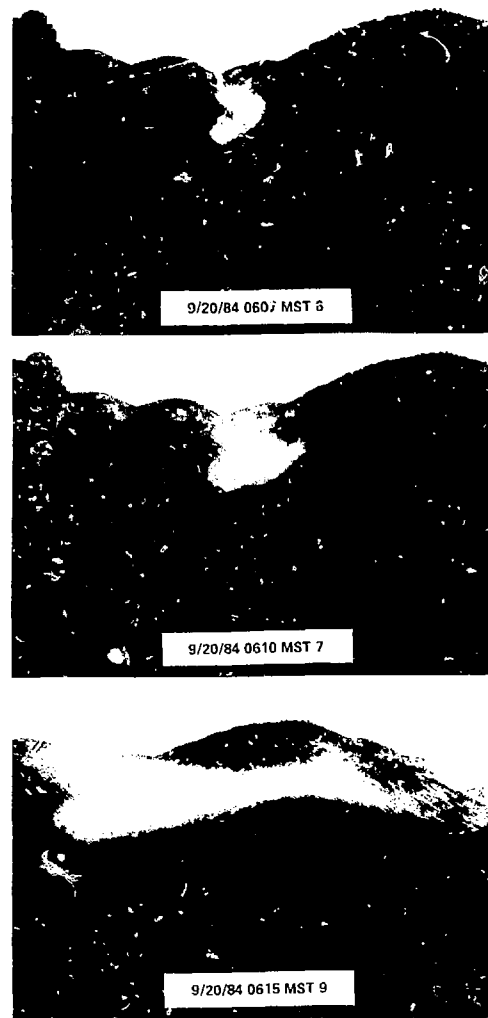


Figure 4. Views of the dispersion of oil fog, released on the mesa above the Brush Creek valley, as it descends into the valley.

the MATHEW/ADPIC models of the dispersion of the oil fog and the perfluorocarbon tracer, shown in Fig. 5, provide the qualitatively reasonable tracer distribution one hour after the initiation of the release. A more quantitative analysis between the calculated and measured perfluorocarbon tracer concentrations will be performed as soon as the measured values become available.

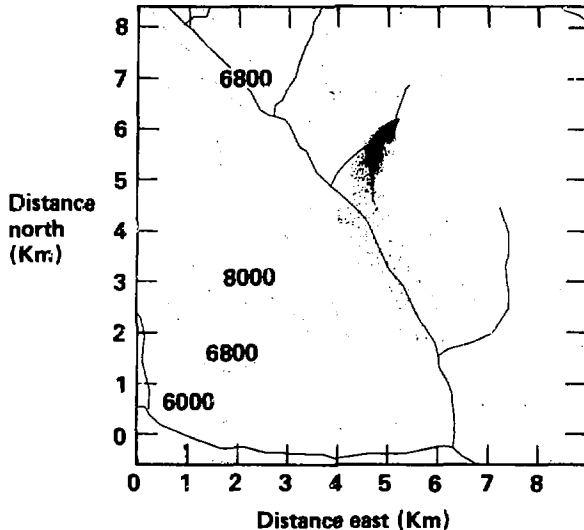


Figure 5. A MATHEW/ADPIC model simulation of the oil fog tracer shown in Fig. 4.

#### THE ARAC PROJECT

The Atmospheric Release Advisory Capability utilizes the MATHEW/ADPIC models to provide predictions of dose levels and the extent of surface contamination from an accidental release of radioactivity into the surface boundary layer of the atmosphere. For global-scale transport and diffusion problems associated with nuclear weapons tests, the 2BUFF, PATRIC, and KDFOC2, models are used.[20,21,22] The ARAC is a Department of Energy sponsored project that supports various federal and state agencies in their role

of protecting public health and safety in the event of accidents at fixed nuclear facilities or transportation incidents that may occur at any location.

The ARAC central operating system, situated at LLNL, integrates data acquisition, data analysis, data-basing and management functions, and atmospheric transport and diffusion models to enable the ARAC staff to produce real-time assessments of an accidental atmospheric release of radioactivity.[23] In order to meet its increasing commitments to the federal and state agencies, it is currently undergoing a significant expansion. This will permit the ARAC to:

- Support up to 100 fixed sites.
- Simultaneously handle two emergency responses.
- Produce preliminary hazards assessments within 15 min of notification at a supported site by the end of 1986.
- Produce enhanced hazards assessments within 45 min of notification and hourly thereafter at a supported site by the middle of 1986.

The preliminary assessment, performed with the MATHEW/ADPIC models, is based on initial accident information, flat terrain, and minimal meteorological information. The enhanced assessment, also performed with the MATHEW/ADPIC models, includes updated source term information, terrain effects, and additional meteorological from supplemented measurement sites.

The ARAC has traditionally used the Lawrence Livermore National Laboratory's central computing facility in conjunction with several minicomputers to perform a hazards assessment of a particular accident. This function is currently being transferred to two ARAC dedicated computers. This includes two dual-processor main computers that are linked with three front-end communications processors, two gigabytes of sharable disk storage, and a telecopier by means of a high-speed local-area communications network. This system, which has been named the ARAC Emergency Response Operating System (AEROS), is capable of interacting directly over commercial telephone lines with the Air

Force Global Weather Central (AFGWC) and a data communications terminal situated at each supported site. This terminal, referred to as the site system, consists of a small professional computer equipped with three modems, a 10-megabyte hard disk, two floppy disk drives, color monitor, keyboard and printer. One of the modems is connected to the site meteorological tower, whereas the remaining two are used to communicate with the ARAC center: one for voice and the other for data transmissions. The system's configuration is shown in Fig. 6. The principal purposes of the site system are to:

- Permit site personnel to transmit meteorological data and accident information to the ARAC center.
- Receive and display ARAC assessments.
- Collect and display local meteorological data.
- Perform localized Gaussian dispersion model calculations.
- Transmit messages to and from the ARAC center.

For supported sites, permanent data bases have been developed for rapid access during an emergency. These include geography, topography, and the locations of meteorological measurement systems. In addition, data describing the nature of potential accidental releases at each site are available at the ARAC center. A schematic diagram of the center's interactions with other organizations during an emergency response is shown in Fig. 7. When notified of an emergency at one of the ARAC serviced sites, the ARAC staff collects information about the nature of the accident directly from the site emergency response personnel. The ARAC personnel also acquires pertinent meteorological data from the site and surrounding region from the AFGWC and the National Weather Service (NWS) and/or Weather Net, as well as from the site itself. Using the AEROS the data are viewed graphically for quality control purposes before initiating the model calculations. Likewise, they carefully screen the model results, which consist of computer-generated displays of radiation dose and surface contamination patterns overlaid on a site map before transmitting them directly to site emergency response personnel. ARAC support to sites that

## ARAC SITE SYSTEM CONFIGURATION

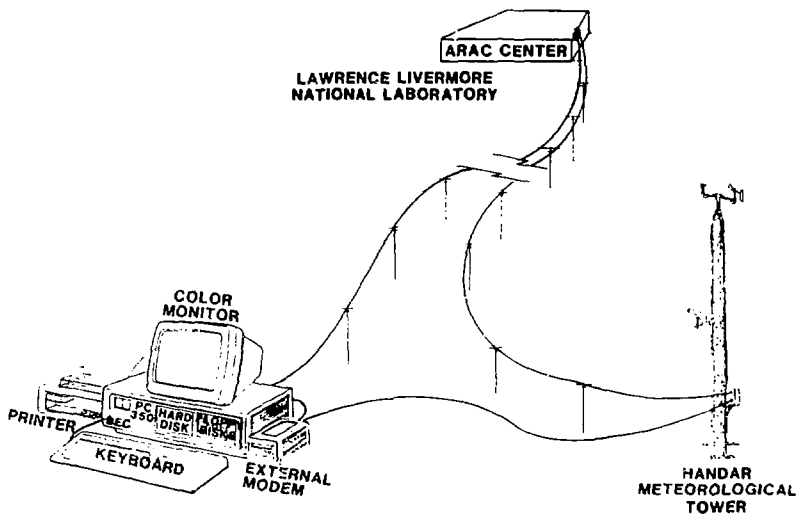


Figure 6. ARAC site system configuration

Table 1. Most Notable ARAC Responses

Listed in Chronological Order

1. Tritium release from the SRP—1974.
2. Train accident involving the potential release of  $UF_6$ —1976.
3. Chinese 200 Kt and 4 Mt atmospheric nuclear weapons tests—1978.
4. Reentry of COSMOS 954 nuclear powered satellite—1978.
5. TMI nuclear power plant accident—1979.
6. TMI purge of Kr-85 from containment—1980.
7. Titan II missile accident—1980.
8. Potential  $H_2S$  leak at the SRP—1981.
9. Ginna nuclear power plant accident—1982.
10. Reentry of COSMOS 1401 nuclear powered satellite—1983.
11. Pershing II missile accident—1984.

are not regularly serviced by ARAC requires a slightly different approach. Meteorological data throughout the region of interest are obtained through the AFGWC computer link, which provides global access to surface and upper-air measurements at approximately 10,000 locations. Measurements near the accident location are obtained by telephone from local authorities. Topographical information for the continental U.S. is extracted from a master terrain data base which was developed from U.S. Geological Survey data tapes, while maps provide geographic data that may be digitized rapidly. These data are then processed in a manner analogous to that of an ARAC-serviced site.

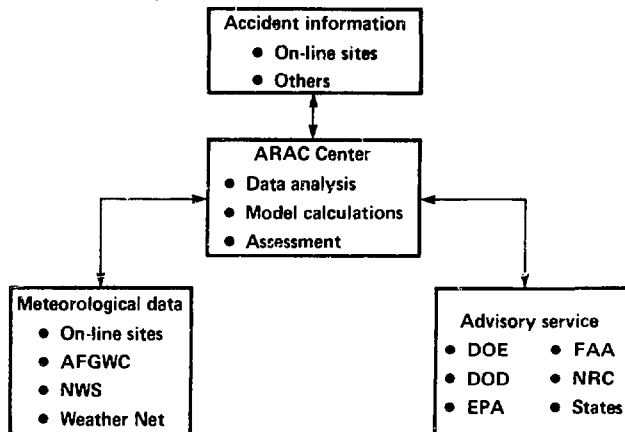


Figure 7. ARAC center functions and interactions.

The ARAC has been involved in over 150 real-and nonreal-time responses during the past decade. These include actual emergencies, alerts, and major exercises. The most notable events are shown in Table 1. These include a wide spectrum of responses associated with actual or potential releases of radioactivity or toxic chemicals from fixed nuclear facilities, transportation accidents, nuclear weapons tests, reentry of nuclear powered satellites, and missile mishaps. Of these the most intensive response was that associated with the TMI accident in 1979. This event required continuous predictions of the radioactive plume

behavior over a roughly two week period. This required two ARAC representatives in the Harrisburg area to interact with the federal emergency response force. The assessments performed by the ARAC staff were used to:

- Provide guidance for the deployment of ground and aerial radiological measurement resources.
- Estimate the amount of radioactivity released in the accident by combining field radiological measurements with model calculations.
- Screen the meteorological and radiological data for consistency.
- Advise federal agencies about the potential consequences of the accident.
- Perform a detailed post accident analysis to determine the total population dose.

#### MODELING OF HEAVY GAS SUBSTANCES

Over the past several years the LLNL has focused a significant effort on improving our capabilities to predict the dispersion of accidental spills of heavier-than-air substances such as liquefied natural gas (LNG). This effort has included both experimental and numerical modeling activities sponsored by the U.S. Department of Energy. Several field experiments involving large spills of LNG, ammonia ( $\text{NH}_3$ ), and nitrogen tetroxide ( $\text{N}_2\text{O}_4$ ) were conducted at China Lake, California and the Nevada Test Site in Nevada.[24] These experiments have provided the data needed to develop a spectrum of modeling capabilities.[4,25] This includes the development of a three-dimensional computer model (FEM3), which is based on the finite element methodology.[4] The model solves the time-dependent conservation equations of mass, momentum, energy, and species and treats turbulence by use of a K-theory submodel. This model is currently undergoing evaluation using data from these field experiments. Due to its complexity and the computational requirements this model is not currently applicable for use in real-time ARAC responses but is being used for various hazards assessments associated with toxic or flammable heavy gases. It

is the intent to use this model as a reference point for the development of a simpler time-dependent model that may be suitable for "quasi" real-time accident response, but whose solution accuracy may be evaluated against this "reference" model.

### FEM3 MODEL DESCRIPTION

The FEM3 model is based on solving the following three-dimensional, time-dependent conservation equations:

$$\frac{\partial(\rho \underline{u})}{\partial t} + \rho \underline{u} \cdot \nabla \underline{u} = -\nabla p + \nabla \cdot (\rho \mathbf{K}^m \cdot \nabla \underline{u}) + (\rho - \rho_h) \underline{g}, \quad (10)$$

$$\nabla \cdot (\rho \underline{u}) = 0, \quad (11)$$

$$\frac{\partial \theta}{\partial t} + \underline{u} \cdot \nabla \theta = \frac{1}{\rho C_p} \nabla \cdot (\rho C_p \mathbf{K}^\theta \cdot \nabla \theta) + \frac{C_{PN} - C_{PA}}{C_p} (\mathbf{K}^\omega \cdot \nabla \omega) \cdot \nabla \theta, \quad (12)$$

$$\frac{\partial \omega}{\partial t} + \underline{u} \cdot \nabla \omega = \frac{1}{\rho} \nabla \cdot (\rho \mathbf{K}^\omega \cdot \nabla \omega), \quad (13)$$

and

$$\rho = \frac{PM}{RT} = \frac{P}{RT} \left( \frac{\omega}{M_N} + \frac{1-\omega}{M_A} \right), \quad (14)$$

$$C_p = C_{PA} + (C_{PN} - C_{PA})\omega, \quad (15)$$

where  $\underline{u} = (u, v, w)$  is the velocity,  $\rho$  is the density of the mixture,  $p$  is the pressure deviation from an adiabatic atmosphere at rest, with corresponding density  $\rho_h$ ,  $\underline{g}$  is the acceleration due to gravity,  $\theta$  is the potential temperature deviation from an adiabatic atmosphere at  $\theta_0$ ,  $\omega$  is the mass fraction of the dispersed species,  $\mathbf{K}^m$ ,  $\mathbf{K}^\theta$ , and  $\mathbf{K}^\omega$  are the eddy diffusion tensors for momentum, energy, and the dispersed species,  $C_{PN}$ ,  $C_{PA}$ , and  $C_p$  are the specific heats for the species, air, and the mixture, respectively. In the equation of state,  $P$  is the absolute pressure,  $R$  is the universal gas constant,  $M_N$ ,  $M_A$  are the molecular weights of the species and air, and  $T$  is the absolute temperature ( $T/(\theta + \theta_0) = (P/P_0)^{R/MC_p}$ ). For problems of current interest, involving heights that are generally within the surface boundary layer, the ratio  $P/P_0$  is nearly equal to unity and hence no distinction is made between the absolute and potential temperature.

The source of the dispersing cloud is defined by injecting an appropriate amount of mass and energy through a predetermined source area (usually on the ground). During vapor injection, the following boundary conditions are imposed:

$$V = V_I \quad \text{for the vertical momentum equation,} \quad (16)$$

and

$$K_v \frac{\partial \omega}{\partial n} = \frac{V_I}{\rho} (1 - \omega) \quad \text{for the species equation,} \quad (17)$$

where  $V_I = (\rho v)_I$  is the mass flux of the vapor being injected. For the temperature equation, consideration of enthalpy balance leads to:

$$K_v \frac{\partial \theta}{\partial n} = \frac{V_I}{\rho} \left( \frac{C_P N}{C_P} \theta_N - \theta \right). \quad (18)$$

The eddy diffusion tensors  $\mathbf{K}^m$ ,  $\mathbf{K}^\theta$ , and  $\mathbf{K}^\omega$  are assumed to be diagonal and it is further assumed that  $\mathbf{K}^\theta = \mathbf{K}^\omega$ . The vertical and horizontal diffusion coefficients are given respectively by:

$$\frac{K_V = k[(u_* z)^2 + (w_* l)^2]^{1/2}}{\phi} \quad (19)$$

and

$$K_h = \beta k u_* z / \phi \quad (20)$$

In the above equations,  $u_*$  is the local "friction velocity" incorporating the effects of the ambient and the resulting velocity field,  $w_*$  is the "convection velocity" due to ground heating of the vapor cloud, and  $\phi$  is the Monin-Obukhov profile function given by Dyer [26]. Specifically,  $\phi$  is defined as

$$\phi = 1 + 5Ri, \quad Ri \geq 0 \quad (21a)$$

for all three (momentum, energy, and species) diffusion coefficients, and

$$\phi = \begin{cases} (1 - 16Ri)^{-1/4} & \text{for momentum,} \\ (1 - 16Ri)^{-1/2} & \text{for energy and species} \end{cases} \quad Ri < 0 \quad (21b)$$

The local Richardson number is, in turn, defined as

$$Ri = u_*^2 \frac{Ri_a}{(u_*^2 + w_*^2)} + 0.05 \frac{(\rho - \rho_a)}{\rho} \cdot \frac{gl}{(u_*^2 + w_*^2)} \quad (22)$$

Herein the first term is designed to include the turbulence in the ambient atmosphere and the second term represents the effects of density stratification, generally a reduction of turbulence in the stably stratified, dense vapor cloud.  $Ri_a$  and  $\rho_a$  are the Richardson number and density of the ambient atmosphere. The ambient density is obtained via equation (5) and the ambient Richardson number is defined as

$$Ri_a = z/L \quad (23)$$

where  $z$  is the height above ground and  $L$  is the Monin-Obukhov length scale.

#### FEM3 MODEL EVALUATION

The FEM3 model has been evaluated on the basis of data acquired by the liquid spill experiments. Of principal interest in this paper is the Burro-8 LNG spill test conducted at the China Lake, California test facility. This test consisted of releasing 28.4 m<sup>3</sup> of LNG at a rate of 16 m<sup>3</sup>/min over a shallow pond that measured about 50 m on a side. The surrounding terrain may be characterized as relatively flat with variations of the order of a few meters. The release occurred during slightly stable atmospheric conditions when the surface wind speed was 1.8 m/s at a height of 2 m. This test is especially interesting because the very low wind speed and the high spill rate permitted the gravity flow of the cold, dense vapor cloud to become so dominant that the flow surrounding the cloud was almost decoupled from the ambient atmospheric boundary layer. The cloud spread in all directions, including upwind, developed a very distinct bifurcated structure, and lingered over the source region for more than 100 seconds after the spill was terminated.

The model simulation of the concentration distribution of the natural gas vapor at 180 s for a height of one meter above the ground may be compared with the corresponding measured distribution in Fig. 8. The simulation appears to be in reasonable agreement

with the measurements with regard to the spatial distribution of the concentration pattern even though some of the individual concentration contours differ somewhat. Note the considerable bifurcation in the measured distribution which also clearly appears in the model simulation. This bifurcation is primarily due to heavy gas and terrain effects. The maximum predicted concentration as a function of downwind distance may be compared with the measurements in Fig. 9. Again reasonable agreement may be noted even though the calculated concentrations are slightly lower than those measured. In order to understand the dynamics of the dispersion processes, it is of interest to study the calculated concentration and velocity distributions within the natural gas vapor cloud and its immediate surroundings as shown in Fig. 10. Note in Fig. 10a the outward moving vortex which is formed due to gravity spreading of the vapor cloud in the crosswind direction. The maximum lateral velocity is slightly over 1 m/s, which is about one-half of the ambient wind speed. Superimposed on the velocity vectors are the concentration contours. This figure clearly shows how air is entrained from the top surface into the vapor cloud and also explains how a "nose shape" region near the advancing front of the vapor cloud is formed. Fig. 10b shows the concentration contours and the horizontal component of the velocity on a plane 1 m above the ground at the same time. Profound changes of the velocity field in the source region (from the originally unidirectional velocity field) is apparent and the concentration contours manifest clearly the gravity spreading of the cloud in all directions, including upwind. Furthermore, cloud bifurcation on this plane is also displayed. Thus, on the basis of the above as well as simulations of the other field experiments[25], the model seems to have the capability to simulate the dispersion of heavy gas spills with quite satisfactory accuracy.

The FEM3 model is currently being used to assess the potential hazards associated with storing in excess of 10,000 gallons of liquid chlorine at a sewage treatment plant situated near the San Francisco Bay. Since a high density housing development is planned to be built within 400 m of the chlorine storage tanks, some concern has been voiced in

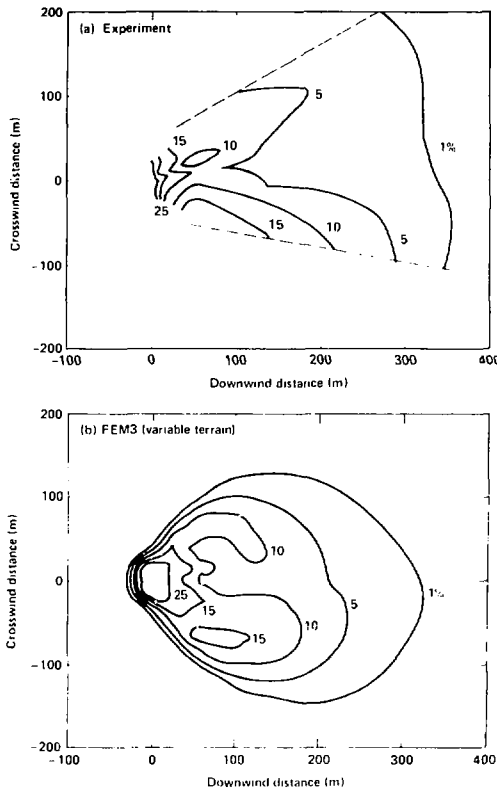


Figure 8. The Burro 8 natural gas volumetric concentration contours 1 m above the ground at  $t = 180\text{ s}$  (a) experiment, and (b) FEM3 computed values.

regard to the safety of the inhabitants of the housing units in the event of an accidental spill of the chlorine. For emergency response planning purposes, a maximum credible accident has been defined as one involving the release of about 9500 gallons of chlorine over a period of a few minutes due to a massive tank rupture caused by a severe earthquake. In the event of such a spill, one may estimate that the cold liquid will flow out on the ground to produce a pool of liquid covering an area of about  $1000\text{ m}^2$  to a depth of a few centimeters. Initially about 15–20% of the liquid will flash into vapor to be dispersed

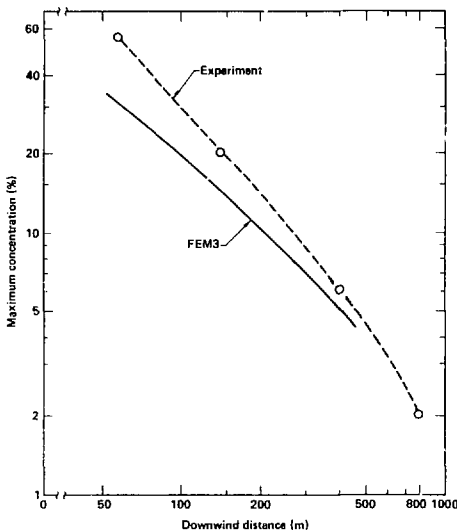


Figure 9. Experimentally observed and FEM3 computed Burro 8 natural gas concentrations as a function of downwind distance.

by the ambient winds. The remainder of the liquid will evaporate over a longer period of time depending on the surface area of the pool, the vapor pressure of the chlorine, and the ambient temperature and winds. By using standard numerical techniques, one may estimate the most likely release rate to be approximately 7.2 kg/s.

Assuming a surface wind speed of 3.5 m/s and neutral atmospheric stability, the FEM3 model predicted the downwind air concentrations due to the pool evaporation to follow the center curve in Fig. 11 out to a distance of about 1 km from the release point. Note that the concentrations at all range considerably exceed the 25 ppm where noticeable health effects may occur even for very short exposure times. Since the spill rate is not well defined under such conditions, we have attempted to bracket the most reasonable variations of the accident scenario by varying the source term by a factor of three. The results of these calculations are also shown in Fig. 11. Note that even for the low spill rate, the chlorine

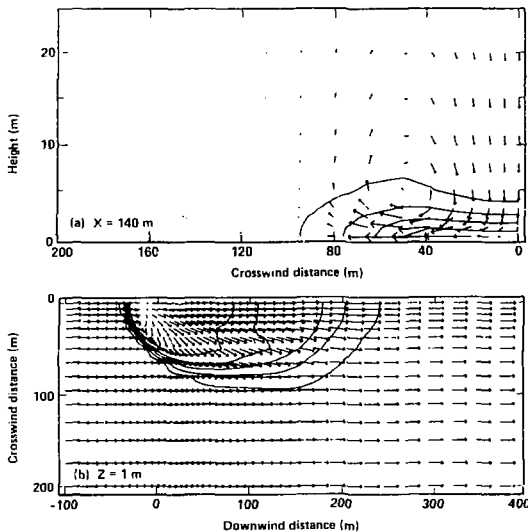


Figure 10. Durro 8 natural gas concentration contours and velocity vectors at  $t = 120$  s  
 (a) 140 m downwind, (b) 1 m above the ground.

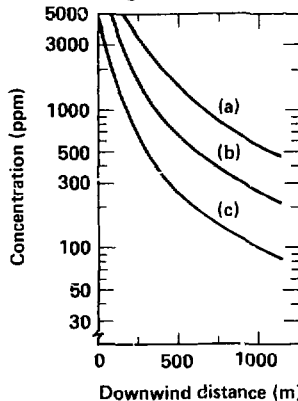


Figure 11. FEM3 computed maximum chlorine concentrations as a function of downwind distance from a hypothetical release. The release rates are: (a) 21.6 kg/s, (b) 7.2 kg/s, and (c) 2.4 kg/s.

concentrations are still about 100 ppm at roughly 1 km from the release point. Hence,

such an event, even though it is highly unlikely to ever occur, could cause significant health effects to nearby residents.

#### SUMMARY

The MATHEW/ADPIC models have undergone extensive evaluation of their capability for simulating pollutant transport and diffusion for a wide spectrum of meteorological and terrain situations. Simulations of numerous tracer experiments reveal that the calculated concentrations are within a factor of 2 for 50% of the measurements for near surface releases in relatively flat terrain, while only 20% of the comparisons are within a factor of 2 for elevated releases in complex terrain.

These models serve as an integral part of the ARAC emergency response service to provide real-time assessments of accidental releases of radioactivity into the atmosphere. It consists of a centralized computer based emergency response system that is capable of supporting up to 100 sites as well as perform assessments of transportation accidents that may occur at any location. In the event of an emergency, the central operating system, situated at LLNL, acquires and integrates the appropriate accident information, local and regional meteorological data and terrain data to permit the staff to execute the model calculations needed to define the hazards to nearby population centers. It has been involved in over 150 real-and non-real-time responses during the past decade.

To predict the dispersion of heavier-than-air gases from accidental spills, a three-dimensional model (FEM3) has been developed. It utilizes a finite element methodology to solve the time-dependent conservation equations of mass, momentum, energy and species, and includes a K-theory parameterization of atmospheric turbulence. The model has been evaluated against several field experiments involving the release of heavy gases, and seems to provide very satisfactory simulations of the spatial and temporal distributions of the test gases with most cases assessed within a kilometer of the release point.

This work was performed under the auspices of the U.S. Department of Energy by the Lawrence Livermore National Laboratory under contract No. W-7405-Eng-48.

## REFERENCES

1. C. S. Sherman, "A Mass-Consistent Model for Wind Fields Over Complex Terrain," *J. Appl. Meteor.*, 17,312-319 (1978).
2. R. Lange, "ADPIC—A Three-Dimensional Particle-in-Cell Model for the Dispersal of Atmospheric Pollutants and Its Comparison to Regional Tracer Studies." *J. Appl. Meteor.*, 320-329(1978).
3. M. H. Dickerson, P.H. Gudiksen, T.J. Sullivan, and G.D. Greenly, "ARAC Status Report: 1985," Lawrence Livermore National Laboratory Report, UCRL-53641 (1985).
4. S. T. Chan, "FEM3—A Finite Element Model for the Simulation of Heavy Gas Dispersion and Incompressible Flow: User's Manual," Lawrence Livermore National Laboratory Report, UCRL-53397 (1983).
5. R. Lange, "A Three-Dimensional Computer Code for the Study of Pollutant Dispersal and Deposition Under Complex Terrain Conditions," Lawrence Livermore National Laboratory Report UCRL-51462 (1973).
6. R. R. Draxler, "Determination of Atmospheric Diffusion Parameters," *Atmos. Environ.*, 10, 99-105 (1976).
7. J. J. Walton, "Scale-Dependent Diffusion," *J. Appl. Met.*, 12, 547-549 (1973).
8. C. H. B. Priestly, "Turbulent Transfer in the Lower Atmosphere," Chicago Univ. Press, 130 pp. (1959).
9. J. A. Businger, J. C. Wyngaard, Y. Izumi and E. F. Bradley, "Flux Profile Relationships in the Atmospheric Surface Layer," *J. Atmos. Sci.*, 28,181-189 (1971).
10. J. A. Businger and S. P. S. Arya, "Height of the Mixed Layer in the Stably Stratified Planetary Boundary Layer," *Advances in Geophysics*, Academic Press, 18A, 73-92 (1974).
11. M. H. Dickerson, "Summary of MATHEW/ADPIC Model Evaluation Studies." Lawrence Livermore National Laboratory Report UCRL-92319, to be published in proceedings

of International Symposium on Emergency Planning and Preparedness for Nuclear Facilities, November 4-8, 1985, Rome, Italy (1985).

12. R. Lange, "ADPIC—A three-dimensional Particle-in-Cell Model for the Dispersal of Atmospheric Pollutants and its Comparison to Regional Tracer Studies," *J. Appl. Meteor.*, 17, 320-329 (1978).
13. M. H. Dickerson, P. H. Gudiksen, and T. J. Sullivan, "The Atmospheric Release Advisory Capability," Lawrence Livermore National Laboratory Report UCRL-52802-83 (1983).
14. K. R. Peterson and R. Lange, "An evaluation and sensitivity study of the MATHEW/ADPIC models using EPRI plains site data for a tall stack," Lawrence Livermore National Laboratory Report UCRL-91856 (1984).
15. R. Lange, "Relationship between model complexity and data base quality for complex terrain tracer experiments," Ph.D. dissertation (1985).
16. P. H. Gudiksen, M. R. Dickerson, R. Lange, and J. B. Knox, "Atmospheric Field Experiments for Evaluating Pollutant Transport and Dispersion in Complex Terrain," Air Pollution Modeling and Its Application IV, pp.507-527, Plenum Press, New York, NY (1985).
17. D. J. Rodriguez, and L. C. Rosen, "An Evaluation of a Series of SF<sub>6</sub> Tracer Releases using the MATHEW/ADPIC model," Lawrence Livermore National Laboratory Report UCRL-91854 (1984).
18. F. Desiato, and R. Lange, "A sea-breeze tracer study with the MATHEW/ADPIC transport and diffusion model," IAEA-SM-280/A2 (prepared for presentation to International Atomic Energy Symposium on Emergency Planning and Preparedness for Nuclear Facilities, Rome, Italy, November 4-8, 1985) (1985).
19. P. H. Gudiksen, M. H. Dickerson, and T. Yamada, "ASCOT FY-1984 Progress Report," Lawrence Livermore National Laboratory UCID-18878-84 (1984).

20. T. V. Crawford, "A Computer Program for Calculating the Atmospheric Dispersion of Large Clouds," Lawrence Livermore National Laboratory Report UCRL-50179 (1966).
21. R. Lange, "PATRIC, A Three-Dimensional Particle-in-Cell Sequential Puff Code for Modeling the Transport and Diffusion of Atmospheric Pollutants," Lawrence Livermore National Laboratory Report UCID-17701 (1978).
22. T. F. Harvey and F. J. D. Serduke, "Fallout Model for System Studies," Lawrence Livermore National Laboratory Report UCRL-52858 (1979).
23. T. J. Sullivan and S. S. Taylor, "A Computerized Radiological Emergency Response and Assessment System," to be published in proceedings of International Symposium on Emergency Planning and Preparedness for Nuclear Facilities, November 4-8, 1985, Rome, Italy (1985).
24. R. P. Koopman, "A Facility for Large-Scale Hazardous Gas Testing Including Recent Test Results," Lawrence Livermore National Laboratory Report UCRL-93424, presented at The Hazardous Materials Management Conference and Exhibition, December 3-5, 1985, Long Beach, California (1985).
25. D. L. Ermak and S. T. Chan, "A Study of Heavy Gas Effects on the Atmospheric Dispersion of Dense Gases," Lawrence Livermore National Laboratory Report UCRL-92494, presented at the 15th International Technical Meeting on Air Pollution Modeling and Its Application, April 15-19, 1985, St. Louis, MO (1985).
26. A. J. Dyer, "A Review of Flux-Profile Relationships," *Boundary-Layer Met.*, 7, 363-372 (1974).